Colorimetric Determination of Triacetin in Polymer-Composites

ARTICLE *in* JOURNAL OF COMPUTATIONAL AND THEORETICAL NANOSCIENCE · FEBRUARY 2012

Impact Factor: 1.34 · DOI: 10.1166/asl.2012.1990

Langmuir

ARTICLE

pubs.acs.org/Langmuir

Polymerization Model for Hydrogen Peroxide Initiated Synthesis of Polypyrrole Nanoparticles

Karolis Leonavicius,[†] Almira Ramanaviciene,[‡] and Arunas Ramanavicius*[,†,§]

[†]Department of Physical Chemistry and [‡]NanoTechnas—Centre of Nanotechnology and Material Science, Faculty of Chemistry, Vilnius University, Naugarduko 24, LT-03225 Vilnius 6, Lithuania

[§]Department of Materials Science and Electronics, Institute of Semiconductor Physics, State Scientific Research Institute Centre for Physical Sciences and Technology, Vilnius, Lithuania

ABSTRACT: A very simple, environmentally friendly, one-step oxidative polymerization route to fabricate polypyrrole (Ppy) nanoparticles of fixed size and morphology was developed and investigated. The herein proposed method is based on the application of sodium dodecyl sulfate and hydrogen peroxide, both easily degradable and cheap materials. The polymerization reaction is performed on 24 h time scale under standard conditions. We monitored a polaronic peak at 465 nm and estimated nanoparticle concentration during various stages of the reaction. Using this data we proposed a mechanism for Ppy nanoparticle formation in accordance with earlier emulsion polymerization mechanisms. Rates of various steps in the polymerization mechanism were accounted for and the resulting particles identified using atomic force microscopy. Application of Ppy nanoparticles prepared by the route presented here seems very promising for biomedical applications where biocompatibility is paramount. In addition, this kind of synthesis could be suitable for the development of solar cells, where very pure and low-cost conducting polymers are required.

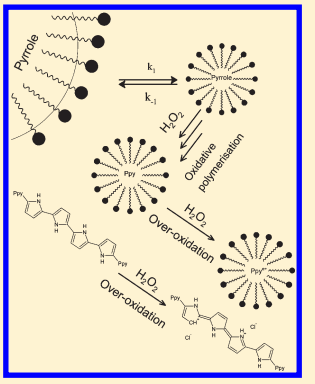

1. INTRODUCTION

Conducting polymer polypyrrole is very often applied for the development of new multifunctional nanomaterials, which are used for various applications. There are some signs that polypyrrole nanoparticles may find some biomedical applications because Ppy exhibits compatibility toward proteins,[1,2] DNA,[3,4] and real biocompatibility toward endothelial cells.[5] Moreover, Ppy nanoparticles show true biocompatibility in vivo since they do not irritate the immune system of mammalians.[6] In addition to other useful properties, Ppy offers attractive actuating properties[7] and it is relatively stabile at atmospheric conditions. Hollow polypyrrole-based containers with regulated uptake/release properties[8] or suitable for encapsulation of fluorescent dyes[9] could be formed; therefore, Ppy could be applied in controlled drug release systems. Moreover, polypyrrole could have been applied for modification of inorganic nanoparticles as a layer suitable for further modifications.[10] To enhance its biological recognition functions Ppy might be easily modified by inorganic materials and by proteins,[10,11] DNA,[12] and molecular imprints.[13] It was shown that Ppy is very suitable for the development of scaffolds for tissue engineering.[14] For these and many other reasons, the Ppy seems a superior material for the creation of various biomedical devices, drug delivery systems, and other nanomedications.[15]

A number of methods for preparation of conducting polymer polypyrrole have been reported during recent years, including electrochemical polymerization, chemical polymerization, and UV-induced radical polymerization.[16] Chemically polypyrrole can be synthesized in various ways: by oxidative synthesis under "harsh" oxidative conditions, by oxidative synthesis under relatively "mild" conditions where redox enzymes are applied,[17] and by oxidative synthesis at ionic-liquid/air interface.[18]

The majority of currently used Ppy formation methods use strong oxidants (e.g., $FeCl_3$, $KMnO_4$, $K_2Cr_2O_7$, etc.). In this type of synthesis, the Ppy is doped with the ions of oxidant, products, and/or other materials that are added into the solution used for polymerization. For this reason, biomedical application of such Ppy particles might be problematic due to traces of toxic materials present in the formed polymer, which become entrapped during the course of polymerization.

Specific biochemical methods suitable for the enzymatic production of conducting polymers including polypyrrole[19,20] and polyaniline[21] were reported and they are under continuous interest. These methods are based on oxidative synthesis under mild conditions where redox enzymes are applied to generate hydrogen peroxide as the oxidant, which then carries out polymerization of the corresponding conducting polymer; it allows adjustment and optimization of analytical parameters of biosensors.[17] Alternatively, the formation of Ppy nanoparticles of different size is possible by the variation of duration of the polymerization reaction.[22] Such Ppy nanoparticles as well as nanoparticles of other conducting polymers have attracted considerable attention within recent years because of their potential applications in various areas, such as drug delivery,[23] electrochemical sensors,[24]

Received: February 18, 2011
Revised: July 7, 2011
Published: July 11, 2011

Scheme 1. The Most Important Steps in Formation of Ppy Nanoparticles

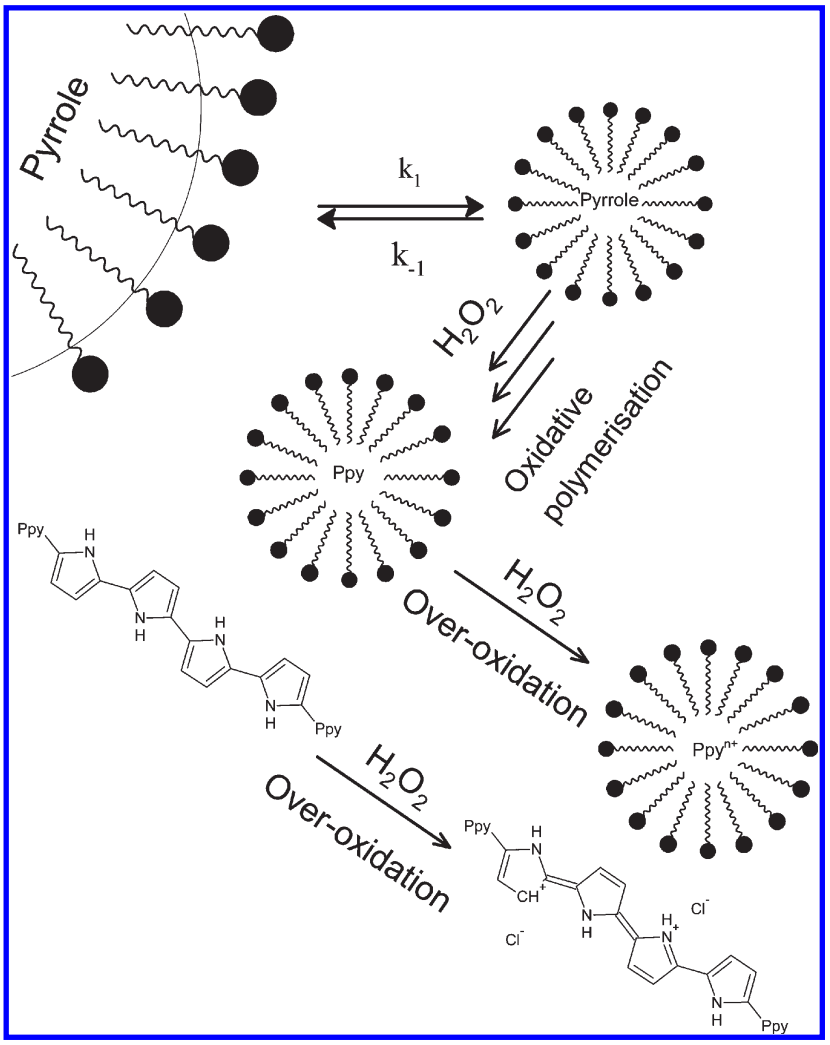

fluorescence-quenching based biosensors,[25] nanoscale electronics,[26] optoelectronics, and electromechanical devices.[27]

Many mentioned applications need very pure Ppy, which is not usually achieved when oxidants used in the synthesis (e.g., $FeCl_3$; $KMnO_4$; $K_2Cr_2O_7$) remain entrapped within formed Ppy structures. To solve the mentioned problems and to prepare pure Ppy nanoparticles, the H_2O_2 could be a very suitable oxidant for the synthesis of Ppy. The H_2O_2 can be easily removed from the formed polymer, since it is not charged and does not form any ionic interactions within highly ionized Ppy matrix, as is the case with ionic oxidants, e.g., $FeCl_3$, $KMnO_4$, $K_2Cr_2O_7$. Moreover, the unreacted H_2O_2 degrades relatively quickly to H_2O and O_2. According to our best knowledge, there is only one research work where H_2O_2 was used for the synthesis of Ppy nanoparticles together with Fe^{3+}.[28] Iron, although not a toxic metal, still presents danger for the cellular environment due to the same radical reactions, as the authors used it for initiation of polymerization. On the other hand, entrapped Fe^{3+} and Fe^{2+} ions significantly reduce photostability of formed Ppy.

The aim of the present study is the preparation of Ppy nanoparticles by oxidative H_2O_2 initiated polymerization and evaluation of the influence of detergent sodium dodecyl sulfate (SDS) concentration on the size, morphology, polymerization rate, and mechanism of Ppy nanoparticle formation. The novelty of our work is in using a completely Fe^{3+} ion free polymerization environment.

2. EXPERIMENTAL SECTION

2.1. Materials and Equipment. Pyrrole, HCl, hydrogen peroxide, and SDS were purchased from Sigma (Darmstadt, Germany) and were used as received. A UV−vis spectrometer (Lambda-25, Perkin-Elmer, Shelton, CT) was used for spectrophotometric measurements. Plastic disposable UV−vis cuvettes were used in the spectroscopic measurements.

2.2. Preparation of Ppy Nanoparticles. To prepare polypyrrole nanoparticles we have developed the following emulsion polymerization procedure: polymerization was performed in 1.0 mL reaction solution, which consisted of 40 mM HCl and 290 mM pyrrole and contained from 0 to 450 mM SDS. The concentration of SDS was varied to find out its influence. We did not use any pH-stabilizing buffer to avoid increasing the ionic strength, and SDS itself was buffering the pH at a constant value of 3.1 during the polymerization reaction. The polymerization solution was stirred for a minute at 2500 rpm before addition of 390 mM hydrogen peroxide. Immediately after the addition of hydrogen peroxide, the solution was stirred again for 5−10 s, and then the UV−vis absorption

dx.doi.org/10.1021/la201962a |*Langmuir* 2011, 27, 10970–10976

Scheme 2. Transformation of Ppy in Presence of H_2O_2 and in Acidic/Alkaline Media

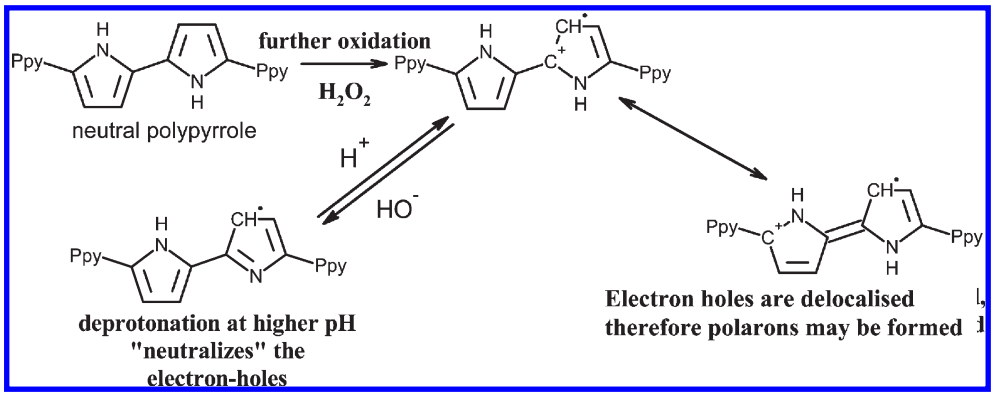

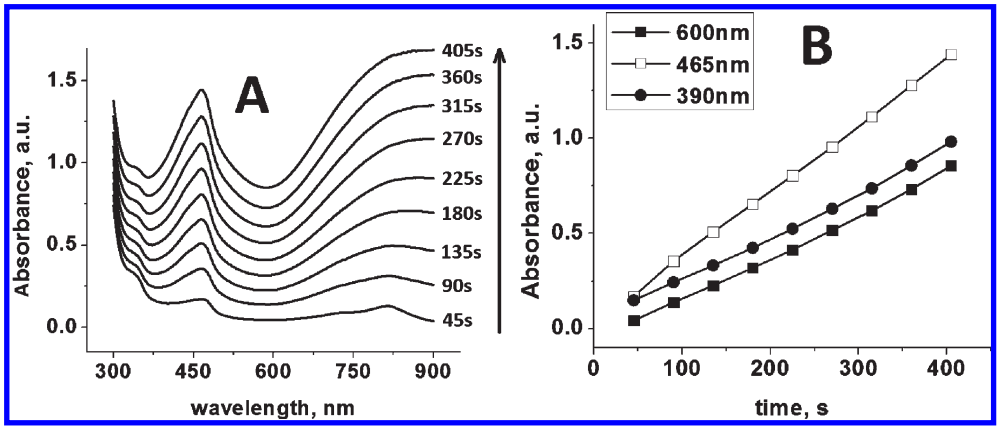

Figure 1. Changes of optical absorption during the polymerization of pyrrole, in a solution consisting of 290 mM pyrrole, 40 mM HCl, and 0.1 M SDS, measured every 45 s. (A) Absorbance spectra after different periods of polymerization and (B) absorbance at different wavelengths (600, 468, 390 nm) vs duration of polymerization.

was monitored in plastic disposable cuvettes of 1 cm optical path. Afterward, the solution was left for 24 h to complete the polymerization.

2.3. Atomic Force Microscopy and Scanning Electron Microscopy Imaging. The 10 μL of resulting Ppy colloid solution after 24 h polymerization period was mixed with 10 μL of 0.1 M SDS solution and diluted by 980 μL of water. A 4 μL droplet of this solution was placed on a glass slide and dried.

The size and morphology of the formed Ppy nanoparticles were examined using an atomic force microscope (AFM) (Bioscope II, Veeco, Santa Barbara, CA) in tapping mode. The RTESP model cantilevers based on phosphorus-doped silicon (1−10 Ω cm^{-1}, k = 20−80 N/m, f_0 = 261−297 kHz) were received from Veeco and were used for AFM measurements.

Scanning electron microscopy (SEM) imaging of Ppy nanoparticles dispersed on conducting carbon substrate was performed by scanning electron microscopy (JSM-7500F from JEOL Ltd., Tokyo, Japan).

2.4. Spectrophotometric Study of Ppy Nanoparticles. The dependence of Ppy nanoparticles optical absorption spectra on pH and ionic strength was analyzed. The 10 μL of resulting Ppy colloid solution after 24 h polymerization period prepared in 0.1 M SDS was mixed with 10 μL of 0.1 M SDS solution and diluted with water to obtain 10 mL of final solution. The pH of the solution was changed by dropwise addition of 30% HCl or 3 M NaOH.

2.5. Droplet Size Distribution by Dynamic Light Scattering. Droplet size distribution was determined by dynamic light scattering (DLS) based device Zetasizer ZEN3600 from Malvern Instruments Ltd. (Worcestershire, United Kingdom). The Zetasizer ZEN3600 is equipped with 633 nm "red" laser, and before the measurements, the device was calibrated with polystyrene latex nanoparticles of 60 nm in diameter. Dual angle detection mode based on 173° backscattered and 13° forwardscattered light was applied, and the average value of two scans with interval of 2 min was calculated and evaluated. The DLS measurement was performed in 0.1 M SDS, 40 mM HCl, and 290 mM pyrrole in water.

2.6. Computation and Mathematical Evaluation of Polymerization Results. Maple 11 software from Maplesoft (Ontario, Canada) was used for the mathematical modeling. A set of differential equations as presented in the Results and Discussion was used as a model for the simulation of Ppy polymerization. Lambda-25 software, which was provided with the spectrometer, was used for the calculation of the first derivative of absorbance changes at 465 nm versus duration of polymerization. Numerical solutions were adapted to the experimental spectroscopic results using a trial-and-error approach.

3. RESULTS AND DISCUSSION

3.1. Description of the Proposed Polymerization Mechanism. Three main steps, (i) micelle formation, (ii) oxidative polymerization and (iii) oxidative-doping, are the most important for formation of Ppy nanoparticles (Scheme 1). Further Ppy oxidation leads to structures that are very suitable for polaron formation (Scheme 2). The concept of a polaron formation is

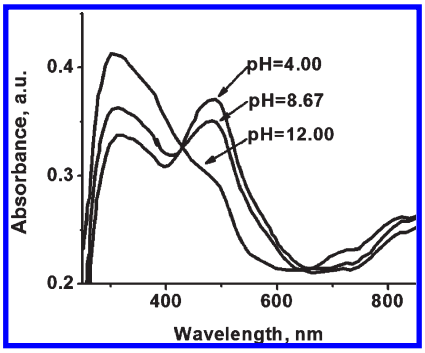

Figure 2. Polypyrrole absorption changes at different pH values.

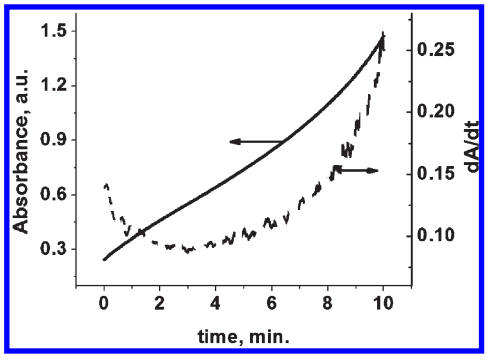

Figure 3. Changes of optical absorption with time in a polymerization solution prepared identically as in Figure 1. The wavelength was fixed at λ = 465 nm. The solid line represents absorbance and the dashed line represents the first-order derivative of absorbance.

central to the investigation of polymerization kinetics[29] evaluated in the present research work. In this context, a polaron is a charge associated with a lattice distortion. It is a very common phenomenon in the case of nanoparticles based on semiconducting materials, which can be easily oxidized or reduced in solutions,[30] and therefore their conductivity increased by doping. The resonance condition is dependent on the electron density in the conductor and the size of the particle. In our case, we observed the absorption peak at 465 nm, which is in agreement with results published by some other authors[31] and our earlier works.[19,20] We used the absorption at 465 nm to measure the arbitrary concentration of nanoparticles.

To investigate the rate of Ppy nanoparticle formation, we measured how the optical absorbance of our samples changes within the first 9 min of polymerization. Figure 1 illustrates how the optical absorbance at different wavelengths depends on polymerization duration. The most important optical absorbance peak at 465 nm indicates that a nanoparticle is fully formed and it becomes oxidatively doped by the excess of H_2O_2. The doping level of the Ppy nanoparticle by H_2O_2 is unknown, but it is assumed to be constant because the concentration and the standard reduction potential of peroxide remain constant during the time frame of polymerization. The oxidation of formed Ppy, protonation/deprotonation mechanisms, and presumptions for polaron formation are presented in Scheme 2. When the pH is increased, the positively charged electron holes are "neutralized,"[32] as is shown in Figure 2. Neutralization of the electron holes decreases the doping level, which decreases the absorption at the polaron wavelength of 465 nm. More detailed analysis of the optical absorption spectra of conductive polymers is available in the literature.[33]

We also investigated how the absorbance changes with respect to time. It is proportional to the concentration of the particles, as once they are formed and oxidatively doped they start absorbing light at 465 nm. The rate of formation of these particles is proportional to the derivative of the absorbance with respect to time. An example plot is shown in Figure 3, which was recorded during polymerization in 0.1 M SDS. In the plot, the smooth and dashed lines (Figure 3) show how absorbance and its derivative change with respect to time. Since the absorbance is proportional to the concentration, the first-order derivative is proportional to the reaction rate. In the presented mathematical model of the particle formation, we assumed that (i) the Beer−Lambert law applies to the particles and (ii) particle oxidation is much faster than the polymerization reaction. At the early stages of polymerization, the presented assumptions are viable and they are good constraints for the development of the particle formation mechanism. The first assumption is correct, as long as we neglect the light scattering and shadow formation, which is possible due to the small size and low concentration of Ppy nanoparticles. The second approximation, which assumes that particle oxidation is much faster than the polymerization reaction, is also true, because for bigger particles the reduction potential is more negative compared with the individual reactant molecules with lower capability of charge distribution. Some other researchers suggest that oxidation of Ppy is a fast process.[33] Comparison with polyaniline nanoparticle formation also suggests that oxidation of the individual monomers but not the oxidation of the polymer is the rate-limiting step.[34]

In the present study, only the first minutes of the polymerization were taken into account, because in later periods the optical absorbance appears to increase very rapidly with respect to time.

Some earlier emulsion polymerization mechanisms were evaluated by some other authors.[35] In addition to this, our research provided useful concepts and background about the emulsion polymerization mechanism. Accordingly, our proposed mechanism consists of several distinct steps that are important for the formation of Ppy nanoparticles. The first step is the formation of big and unreactive droplets of pyrrole, which are formed immediately after the addition of SDS. The surface tension of these droplets is not high enough to react with the hydrogen peroxide, but instead they exist in equilibrium with smaller droplets, of micellar size (20−30 nm), which react rapidly with hydrogen peroxide to form the nanoparticles. The assumptions about droplets in equilibrium are according to a well-accepted microemulsion polymerization mechanism.[36] The size of the small droplets is assumed to be approximately the same size as Ppy nanoparticles, which are backed up by AFM. The size of droplets was determined by dynamic light scattering, and by this experiment, 30 nm and 1.2 μm diameter droplets were clearly observed in the sample (Figure 4).

The equilibrium between the two processes, as illustrated in Scheme 1, is such that it leads to the decrease of the reaction rate, immediately after the addition of peroxide. This shows that the reactive species (small droplets) are being depleted and new steady-state conditions are reached after introduction of hydrogen peroxide. The origin of the high reactivity of the small droplets is due to their small size, which results in a high surface tension. As soon as the small droplets are formed, they react rapidly with the hydrogen peroxide to polymerize and consequently oxidize. Scheme 1 illustrates all of the steps mentioned here. Figure 5 illustrates how the average polymerization rate

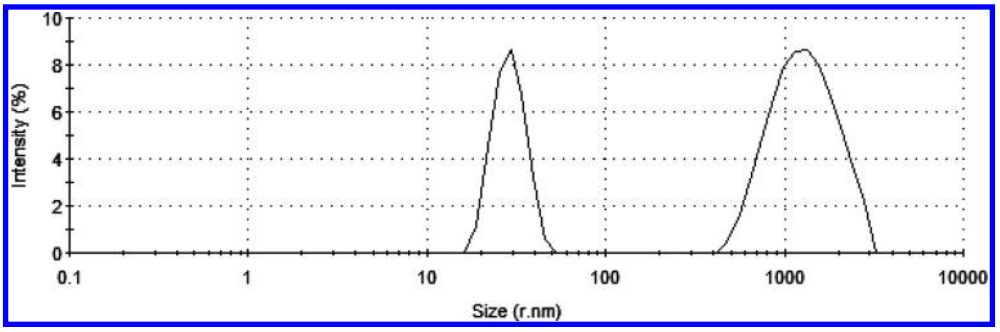

Figure 4. Size distribution by intensity obtained using dynamic light scattering. The measurement was performed in 0.1 M SDS, 40 mM HCl, and 290 mM pyrrole in water.

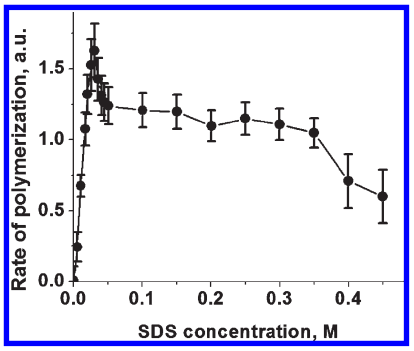

Figure 5. Change in the average polymerization rate at different SDS concentrations.

depends on the concentration of SDS. Main observations are that the polymerization rate is fairly low, when the concentration of SDS is lower than the critical micelle concentration and the formation of smaller droplets is impossible. It was found that the critical micelle concentration of SDS was around 3.3 mM, by linearly extrapolating the first four points of the rate of polymerization vs SDS concentration. When the SDS concentration is increased over 3.3 mM, the mechanism described here starts to apply and the polymerization rate increases rapidly. Further increase in concentration of SDS results in the decrease of the rate as the viscosity of the solution increases and motion of various reactants is impeded.[37] We would like to stress that our goal is investigation of nanoparticle formation, rather than bulk polymerization of pyrrole.[35]

3.2. Mathematical Simulation and Analysis of the Polymerization Reaction. Scheme 1 summarizes the essential steps mentioned before. For the mechanism we considered three distinct species:

(A) big unreactive droplets,
(B) small and reactive droplets,
(C) oxidatively doped polypyrrole product particles.

The three rate constants of interest here are k_1 and k_{-1}, defining the equilibrium between the droplets, and the constant k_2, defining the rate of formation of C. We used a set of differential equations to model the behavior of the system during the first 9 min:

$$\frac{d[A]}{dt} = -k_1[A] + k_{-1}[B] \quad (1)$$

$$\frac{d[B]}{dt} = k_1[A] - k_{-1}[B] - k_2[B] \quad (2)$$

$$\frac{d[C]}{dt} = k_2[B] \quad (3)$$

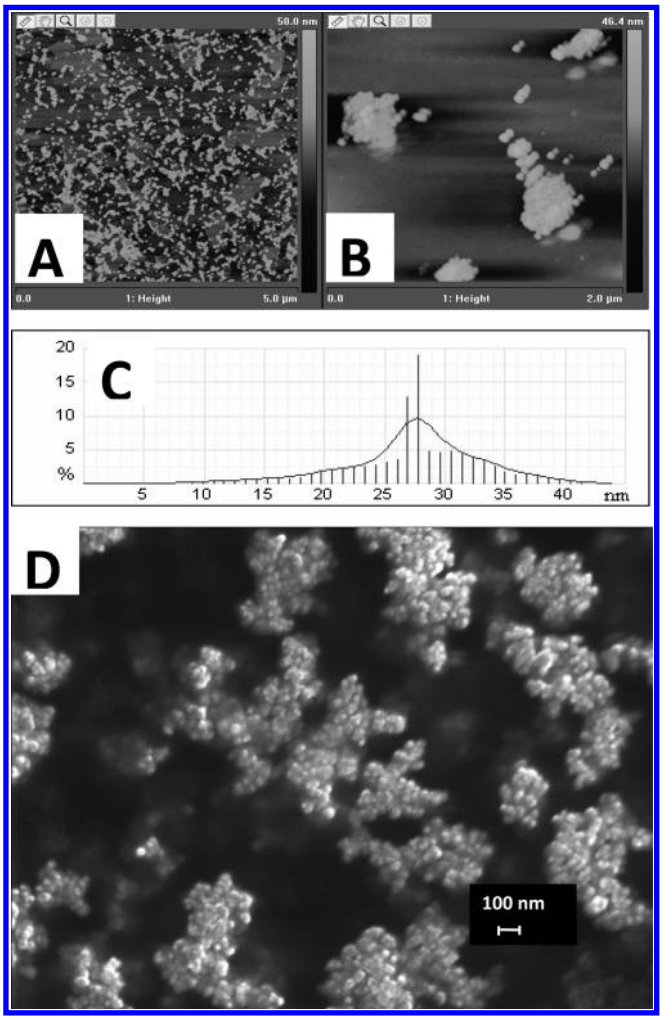

Figure 6. AFM images of the formed polypyrrole nanoparticles with (A) area of 5 × 5 μm and (B) area of 2 × 2 μm. (C) Distribution histogram of their diameters, calculated from image A. (D) Scanning electron microscopy image of Ppy nanoparticles.

The later behavior was accounted for by adding a fitted exponential function, as any kind of mathematical modeling beyond the first 9 min proved to be unreliable.

We estimated peroxide concentration to be constant throughout the reaction time considered, because during the first 9 min less than 1% of the end product was formed. Also the initial concentrations of A and B were calculated by assuming a particle

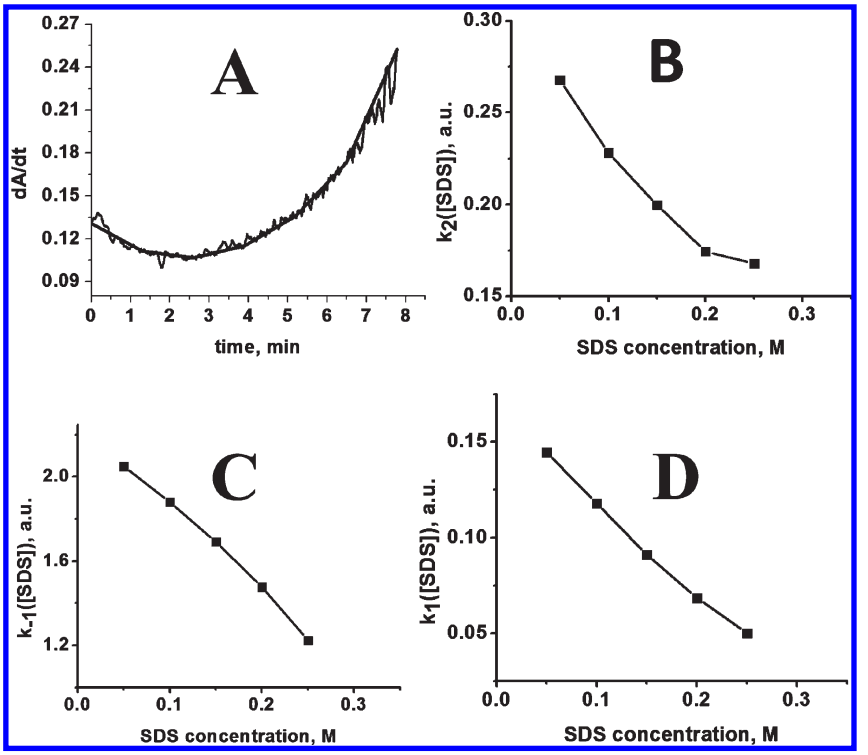

Figure 7. (A) First-order derivative of absorbance. The rate constants calculated from the mathematical model, which was adapted to the experimental data: (B) $k_2[(SDS)]$ vs SDS concentration, (C) $k_{-1}[(SDS)]$ vs SDS concentration, (D) $k_1[(SDS)]$ vs SDS concentration.

size of roughly 1.2 μm[35,36] and 30 nm, as determined by dynamic light scattering (Figure 4) and AFM measurements (Figure 6). The exponential functions were fitted to individual sets of data and the relative magnitudes of the rate constants were determined from the 9 min period. The rate constants were expressed in terms of arbitrary units, because accurate sizes of the monomer droplets were not known.

Figure 7 shows one example of the data fitting to the derivative of the absorbance according to the model above. The same fitting procedure was applied to the polymerization at different SDS concentrations when the rate constants were evaluated. Figure 7 also shows how the three constants vary with SDS concentrations. Simple inspection shows the decrease of all parameters, which is most likely due to the increasing viscosity of the solutions.[37] The constants k_{-1} and k_2 involving [B] (eq 1−3) decrease by half upon the increase of SDS concentration from 0.05 to 0.25 M and the constant k_1 involving [A] decreases to one-third of its initial value. This suggests that the motion of big particles is impeded more than the motion of the smaller ones, which is expected, as diffusion is generally limited by the size of the diffusing species. A final point to make is that the rate constants k_{-1} and k_2 involving [B] are higher than k_1 for the big droplets, which, considering the surface tension, is also a logical outcome.

3.3. Particle Properties in Different Solution Environments. In this work, we were using the concept of polarons as the way of monitoring the particle concentration. To prove the existence of this quantum mechanical effect phenomenon, we measured the UV−vis spectra at different pH. Figure 2 shows that at pH >8.5, the optical absorbance at λ = 465 nm changes rapidly, and at this point the particle color changes from red to green. This point in earlier works has been referred to as the point of transition between insulating and conducting states.[38,39] It can be attributed to the electron holes, which are fundamental charge carriers in PPy and are neutralized by the loss of protons from the polymer, as shown in Scheme 2. The whole process is completely reversible in the time frame of minutes. The slow kinetics of color change suggests that some structural changes are taking place during the changes of pH. Figure 2 shows how the absorption peak at λ = 465 nm devolves with the increase of pH. The influence of ionic strength was also studied, and we have found that particles start to form aggregates when the concentration of sodium chloride increases from 0.05 to 0.5 M and a red solution of Ppy nanoparticles is turned completely colorless with black precipitate. It should be taken into account that formed Ppy nanoparticles have an intrinsic tendency to agglomerate due to their electrostatic and van der Waals interactions arising from their high surface area. Therefore, it has been of both theoretical and practical importance to determine how to make stable conducting polymer nanoparticles with fixed sizes.

3.4. AFM Study of the Ppy Nanoparticles. To investigate the morphology and the size of formed Ppy particles, we used atomic force microscopy. We found that the number of measured/counted particles was around 150 on average in a 1.2 μm^2 area of glass substrate. To increase the accuracy of measurements, the distribution of individual particle sizes was evaluated manually by measuring the diameter of each particle present in the image.

Typical images show spherical and aggregated particles of approximate 28 nm mean diameter (Figure 6A,B). The diameter of Ppy nanoparticles slightly differs from the diameter of Ppy nanoparticles (40 nm), which were formed by initiation of polymerization with $FeCl_3$ in octanol/water emulsion.[27] The samples for AFM imaging were prepared on specialized laboratory glass surface, which was free of inherent surface features that could negatively influence this kind of imaging and interpretation. Therefore, scanning

electron microscopy (SEM) imaging was performed; the SEM image (Figure 6D) confirms that Ppy particles are in the same range. The AFM height distribution diagrams confirm that the diameter of most Ppy nanoparticles is centered around 30 nm (Figure 6C). Using AFM imaging, we have determined that changes in SDS concentration in the range 0.05−0.35 M had no significant influence on the size of Ppy nanoparticles. Moreover, the concentration of SDS did not influence their aggregation and the polaron wavelength, which is attributed to Ppy charge density and particle size. Therefore, it could be concluded that all Ppy nanoparticles were found to be spherical, with 28 nm mean diameter, forming a stable colloid solution.

4. CONCLUSIONS

In this work, we have shown that Ppy could be formed if hydrogen peroxide is applied as an oxidant. The use of H_2O_2 has a number of advantages over other oxidants, since H_2O_2 can be easily removed and/or rapidly degraded after the polymerization reaction. Therefore, in this research, the proposed procedure allows formation of pure Ppy. Furthermore, it uses only cheap and environmentally friendly materials, so it can be scaled for industrial processes. Aspects of the mechanisms of the reaction were evaluated. Spectrophotometric measurements and AFM imaging confirmed the herein proposed early stage polymerization mechanism. Mathematical modeling was applied, and calculations showed the validity of this model at early polymerization stages. Although we could not determine the normalized values of the rate constants for the separate steps, we were able to comment on their relation to each other and to SDS concentration. Eventually, we showed that initial addition of SDS increases the polymerization rate more than 10-fold. The increase of SDS concentration over 0.1 M had no advantages for particle quality.

AUTHOR INFORMATION

Corresponding Author

*E-mail: Arunas.Ramanavicius@chf.vu.lt.

ACKNOWLEDGMENT

This research was funded by a grant (No. MIP-97/2010) and a fellowship for K.L., both provided by the Research Council of Lithuania. The authors are grateful to Česlovas Višnevskij for technical advice related to the application of the Zetasizer.

REFERENCES

(1) Kausaite-Minkstimiene, A.; Mazeiko, V.; Ramanaviciene, A.; Ramanavicius, A. *Biosens. Bioelectron.* **2010**, *26*, 790–797.
(2) O'Grady, M. L.; Parker, K. K. *Langmuir* **2008**, *24* (1), 316–322.
(3) Ramanaviciene, A.; Ramanavicius, A. *Anal. Bioanal. Chem.* **2004**, *379*, 287–293.
(4) Wang, J.; Jiang, M. *Langmuir* **2000**, *16* (5), 2269–2274.
(5) Zhang, Z.; Roy, R.; Dugre, F. J.; Tessier, D.; Dao, L. H. *J. Biomed. Mater. Res.* **2001**, *57*, 63–71.
(6) Ramanaviciene, A.; Kausaite, A.; Tautkus, S.; Ramanavicius, A. *J. Pharm. Pharmacol.* **2007**, *59*, 311–315.
(7) Higgins, M. J.; McGovern, S. T.; Wallace, G. G. *Langmuir* **2009**, *25* (6), 3627–3633.
(8) Parakhonskiy, B.; Andreeva, D.; M'hwald, H.; Shchukin, D. G. *Langmuir* **2009**, *25*, 4780–4786.
(9) Mazur, M. *Langmuir* **2008**, *24*, 10414–10420.
(10) Azioune, A.; Slimane, A. B.; Hamou, L. A.; Pleuvy, A.; Chehimi, M. M. *Langmuir* **2004**, *20*, 3350–3356.
(11) Ramanaviciene, A.; Ramanavicius, A. *Crit. Rev. Anal. Chem.* **2002**, *32*, 245–252.
(12) Ramanaviciene, A.; Ramanavicius, A. *J. Anal. Bioanal. Chem.* **2004**, *379* (2), 287–293.
(13) Ramanaviciene, A.; Finkelsteinas, A.; Ramanavicius, A. *J. Chem. Educ.* **2006**, *83*, 1212–1214.
(14) Lee, J.-W.; Serna, F.; Schmidt, C. E. *Langmuir* **2006**, *22*, 9816–9819.
(15) Ge, D. T.; Tian, X. D.; Qi, R.; Huang, S. Q.; Mu, J.; Hong, S. M.; Ye, S. F.; Zhang, X. M.; Li, D. H.; Shi, W. *Electrochim. Acta* **2009**, *55*, 271–275.
(16) Ramanavicius, A.; Karabanovas, V.; Ramanaviciene, A.; Rotomskis, R. J. *Nanosci. Nanotechnol.* **2009**, *9*, 1909–1915.
(17) Ramanavicius, A.; Kausaite, A.; Ramanaviciene, A. *Analyst* **2008**, *133*, 1083–1089.
(18) Wang, D.; Li, Y.-X.; Shi, Z.; Qin, H.-L.; Wang, L.; Pei, X.-F.; Jin, J. *Langmuir* **2010**, *26* (18), 14405–14408.
(19) Ramanavicius, A.; Kausaite, A.; Ramanaviciene, A. *Sens. Actuators B* **2005**, *111−112*, 532–539.
(20) Ramanavicius, A.; Kausaite, A.; Ramanaviciene, A.; Acaite, J.; Malinauskas, A. *Synth. Met.* **2006**, *156*, 409–413.
(21) Kausaite, A.; Ramanaviciene, A.; Ramanavicius, A. *Polymer* **2009**, *50*, 1846–1851.
(22) Ramanaviciene, A.; Schuhmann, W.; Ramanavicius, A. *Colloids Surf. B* **2006**, *48*, 159–166.
(23) Geetha, S.; Rao, C. R. K.; Vijayan, M.; Trivedi, D. C. *Anal. Chim. Acta* **2006**, *568*, 119–125.
(24) Diab, N.; Schuhmann, W. *Electrochim. Acta* **2001**, *47*, 265–273.
(25) Ramanavicius, A.; Ryskevic, N.; Oztekin, Y.; Kausaite-Minkstimiene, A.; Jursenas, S.; Baniukevic, J.; Kirlyte, J.; Bubniene, U.; Ramanaviciene, A. *Anal. Bioanal. Chem.* **2010**, *398*, 3105–3113.
(26) Berggren, M.; Nilsson, D.; Robinson, N. D. *Nat. Mater.* **2007**, *6*, 3–5.
(27) Kim, S. W.; Cho, H. G.; Park, C. R. *Langmuir* **2009**, *25*, 9030–9036.
(28) Meng, S.; Zhang, Z.; Rouabhia, M. *Synth. Met.* **2010**, *160*, 116–122.
(29) Liu, X.; Gao, K.; Li, Y.; Fu, J.; Wei, J.; Xie, S. *Synth. Met.* **2007**, *157*, 380–385.
(30) Ramanaviciene, A.; Nastajute, G.; Snitka, V.; Kausaite, A.; German, N.; Ramanavicius, A. *Sens. Actuators B* **2009**, *137*, 483–489.
(31) Liu, Y.; Chu, Y.; Yang, L. *Mater. Chem. Phys.* **2006**, *98*, 304–308.
(32) Hwang, J.-H.; Pyo, M. *Synth. Met.* **2007**, *157*, 155–159.
(33) Patil, A. O.; Heeger, A. J.; Wudl, F. *Chem. Rev* **1988**, *88*, 183–200.
(34) Yang, C.; Du, J.; Peng, Q.; Qiao, R.; Chen, W.; Xu, C.; Shuai, Z.; Gao, M. *J. Phys. Chem. B* **2009**, *113*, 5052–5058.
(35) Chern, C. S. *Prog. Polym. Sci.* **2006**, *31*, 443–486.
(36) Zhuang, Y. Q.; Ke, X.; Zhan, X. L.; Luo, Z. H. *Powder Technol.* **2010**, *201*, 146–152.
(37) Patist, A.; Axelberd, T.; Shah, D. O. *J. Colloid Interface Sci.* **1998**, *208*, 259–265.
(38) Kuramoto, N.; Genies, E. M. *Synth. Met.* **1995**, *68*, 191–194.
(39) Kuramoto, N.; Tomita, A. *Polymer* **1997**, *38*, 3055–3058.